

**SUMMARY REPORT:
NASA NNA05CM01G**

**National Center for Atmospheric Research
June 2005**

**TERRA/MOPITT Measurements of Tropospheric
Carbon Monoxide Distributions in Support of INTEX**

Principal Investigator:

D. P. Edwards

*Atmospheric Chemistry Division
National Center for Atmospheric Research
P.O. Box 3000, Boulder CO 80307, USA
Tel: (303) 497-1857, Fax: (303) 497-1492
Email: edwards@ucar.edu*

Co-Investigators:

J. C. Gille, L. K. Emmons, and D. Ziskin
*Atmospheric Chemistry Division
National Center for Atmospheric Research
P.O. Box 3000, Boulder CO 80307, USA*

1 Introduction

This document represents a final report on work completed on the proposal funded by grant NNA05CM01G.

Interaction with the ongoing satellite measurements programs was an important goal of INTEX-A. The Terra/MOPITT instrument had been making global measurements of the tropospheric carbon monoxide (CO) distribution for 4 years, and was in a unique position to provide valuable support during the field campaign. Remote sensing of CO directly addressed the scientific questions motivating the INTEX-A strategy and deployment, and measurement of this gas was rated as being mission critical. CO is an important trace gas in tropospheric chemistry due to its role in determining the atmospheric oxidizing capacity, as an ozone precursor, and as an indicator and tracer of both natural and anthropogenic pollution arising from incomplete combustion. The satellite perspective provided the more general temporal and spatial context to the aircraft and ground-based measurements during the subsequent scientific analysis. We proposed to build on the experience of supplying MOPITT data to previous field campaigns, such as TRACE-P. We provided expedited MOPITT data processing in near real-time, along with basic analysis of the measurements to indicate, where possible, the origin of the CO plumes that impacted the regions of flight operations and other in situ measurement activities. To ensure maximum exploitation of the satellite information, we will also had a scientist in the field to present and interpret the MOPITT data for the INTEX team, and to help ensure its utility in flight planning.

In support of the INTEX-A field campaign deployments in July and August, 2004, the following work was carried out under this grant:

1. Near real-time processing of MOPITT data at NCAR.

Under usual operation, the raw MOPITT data, in the form of instrument counts, are transferred to NCAR from the NASA LaRC DAAC after download from the Terra satellite. These data are accompanied by supplemental files on instrument pointing and geo-location. The Level 0–1 data processing delivers geo-located calibrated instrument radiances from the instrument count data. These are then fed to the Level 2 processor. This algorithm is composed of the following principal components: the radiative transfer forward model which provides a full physical description of the measurements process, a cloud detection module to identify cloudy pixels, and the maximum-likelihood retrieval. The cloud-detection algorithm combines information from the MOPITT radiances with the MODIS operational cloud mask product to determine if the MOPITT pixel is cloud contaminated and whether a retrieval can be performed. The forward model requires supplemental NCEP (National Center Environmental Prediction) atmospheric information which is obtained from the NASA GSFC DAAC. The output of the Level 2 processor are CO total column and mixing ratio profiles reported at seven levels through the troposphere for each geo-located 22 km×22 km pixel. Validation activities show data accuracy to be about 10%. It is important to note that the mixing ratio at a given level reflects the vertical resolution of the measurement as defined by the retrieval averaging kernel and a priori profile [see *Rodgers*, 2000]. These are also reported for each pixel. The Level 0–2 processing normally takes about 4 days due to the time required to stage and transfer the MOPITT and MODIS data and for computer run-time.

In addition to this usual processing stream, we maintained a dedicated second stream during the campaign. After identifying the Pacific, North American, and Atlantic regions of interest to INTEX-A, the corresponding MOPITT count and supplemental data were transferred

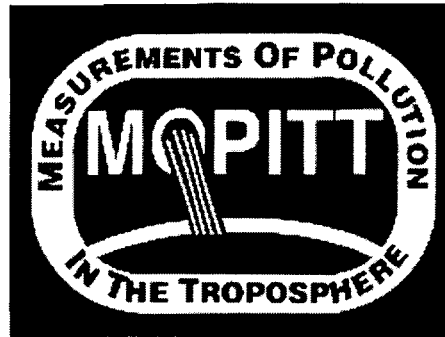
from NASA using an expedited data protocol. Once at NCAR, these were priority-processed. Because of the time required to produce the MODIS cloud mask product, only MOPITT input were used in the cloud detection. This tailored data processing required considerably more data management and programmer attention than regular processing. The total turn-around time between satellite measurement and availability of the Level 2 CO distribution product was about 6 hours. Subsequent to the campaign, these data were reprocessed using the full MOPITT standard system and have been delivered in an easily-used format the the INTEX campaign archive.

2. Maps of the CO distributions for each day for the regions of interest were produced along with several day data-composites. MOPITT uses a cross-track scan, and in the absence of persistent cloud cover, the instrument achieves close to global coverage in 3 days. However, a single day's data are often sufficient to identify CO plumes. These maps, along with the corresponding Level 2 data, were posted to a web-site for easy access by the INTEX team. The website built especially for the INTEX MOPITT project is available at <http://www.eos.ucar.edu/mopitt/INTEX/index.html>. An example of this is shown in Fig. 1. An example mapped CO product is shown in Fig. 2.
3. A scientist at NCAR provided a daily report to accompany the MOPITT product. This included a preliminary analysis of the data, an identification of sources such as burning events, the larger geographical and temporal context to the CO distributions observed in the region of campaign operations, and a comparison with the corresponding observations from previous years to quickly identify significant perturbations from what would normally be expected.
4. Members of the MOPITT science team, Louisa Emmons and Gabrielle Pfister, were present in the field at the flight operations centers during the campaign. These scientists were responsible for receiving the MOPITT CO maps, data, and preliminary analysis and for presenting and explaining this information to the INTEX-A team. In conjunction with other forecast information, the MOPITT data provided useful insight for use in flight planning. We will also helped identify opportunities when Terra overpasses coincided with flights of the DC-8, and conditions allowed for good validation comparisons. Results of these comparisons are currently being evaluated and a journal article is in preparation.
5. Although not directly funded by this grant, work has already been published by our group as members of the INTEX science team detailing inverse modeling studies to obtain estimates of the CO emissions from the intense Alaskan wildfires which had such a large impact on the INTEX campaign region. A reprint of this article from *GRL* is appended.

Pfister, G., P. G. Hess, L. K. Emmons, J.-F. Lamarque, C. Wiedinmyer, D. P. Edwards, G. Petron, J. C. Gille, and G. W. Sachse (2005), Quantifying CO emissions from the 2004 Alaskan wildfires using MOPITT CO data, *Geophys. Res. Lett.*, *32*, L11809, doi:10.1029/2005GL022995.

We present an inverse model analysis to quantify the emissions of wildfires in Alaska and Canada in the summer of 2004 using carbon monoxide (CO) data from the Measurements of Pollution in the Troposphere (MOPITT) remote sensing instrument together with the chemistry transport model MOZART (Model for Ozone and Related Chemical Tracers). We use data assimilation outside the region of the fires to optimally constrain the CO background level and the transport into that region. Inverse modeling is applied locally to quantify the fire emissions. Our a posteriori estimate of the wildfire emissions gives a total of 30 ± 5

Tg CO emitted during June–August 2004 which is of comparable order to the anthropogenic emissions for the continental US. The simulated CO fields have been evaluated by comparison with MOPITT and independent aircraft data.



MOPITT Support for the INTEX Field Campaign

Each Day contains six products:

- Overpass Predictions
- Forecast Images
- Assimilation Images
- Daily Images
- Global 3-Day Images
- INTEX Region 3-Day Images
- Downloadable Data

Additional Materials:

- **Science Log** - highlights features or provides scientific narrative about the data. Updated often.
- **Movies** - animated view of the field project experiment (mpeg format).

May 2004						
Sun	Mon	Tue	Wed	Thu	Fri	Sat
						1
2	3	4	5	6	7	8
9	10	11	12	13	14	15
16	17	18	19	20	<u>21</u>	<u>22</u>

<u>23</u>	<u>24</u>	<u>25</u>	<u>26</u>	<u>27</u>	<u>28</u>	<u>29</u>
<u>30</u>	<u>31</u>					

June 2004						
Sun	Mon	Tue	Wed	Thu	Fri	Sat
		1	2	3	4	5
<u>6</u>	7	8	9	10	11	12
13	14	15	16	17	18	19
20	21	22	23	24	25	<u>26</u>
<u>27</u>	<u>28</u>	<u>29</u>	<u>30</u>			

July 2004						
Sun	Mon	Tue	Wed	Thu	Fri	Sat
				1	2	3
4	5	6	7	8	9	10
<u>11</u>	<u>12</u>	<u>13</u>	<u>14</u>	<u>15</u>	<u>16</u>	<u>17</u>
<u>18</u>	<u>19</u>	<u>20</u>	<u>21</u>	<u>22</u>	<u>23</u>	<u>24</u>
<u>25</u>	<u>26</u>	<u>27</u>	<u>28</u>	<u>29</u>	<u>30</u>	<u>31</u>

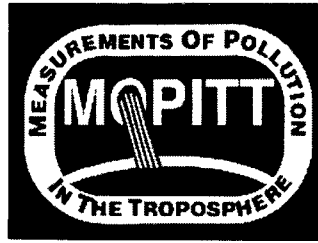
August 2004						
Sun	Mon	Tue	Wed	Thu	Fri	Sat
1	2	3	4	5	6	7
8	9	10	11	12	13	14
15	16	17	18	19	20	21
22	23	24	25	26	27	28
29	30					

CONTACT INFO

NAME	TITLE	PHONE	EMAIL
David Edwards	PI MOPITT INTEX	303-497-1857	edwards@ucar.edu
Daniel Ziskin	MOPITT Data Manager	303-497-2924	ziskin@ucar.edu
Louisa Emmons	INTEX Campaign Scientist	303-497-1491	emmons@ucar.edu
John Gille	MOPITT US PI	303-497-8062	gille@ucar.edu

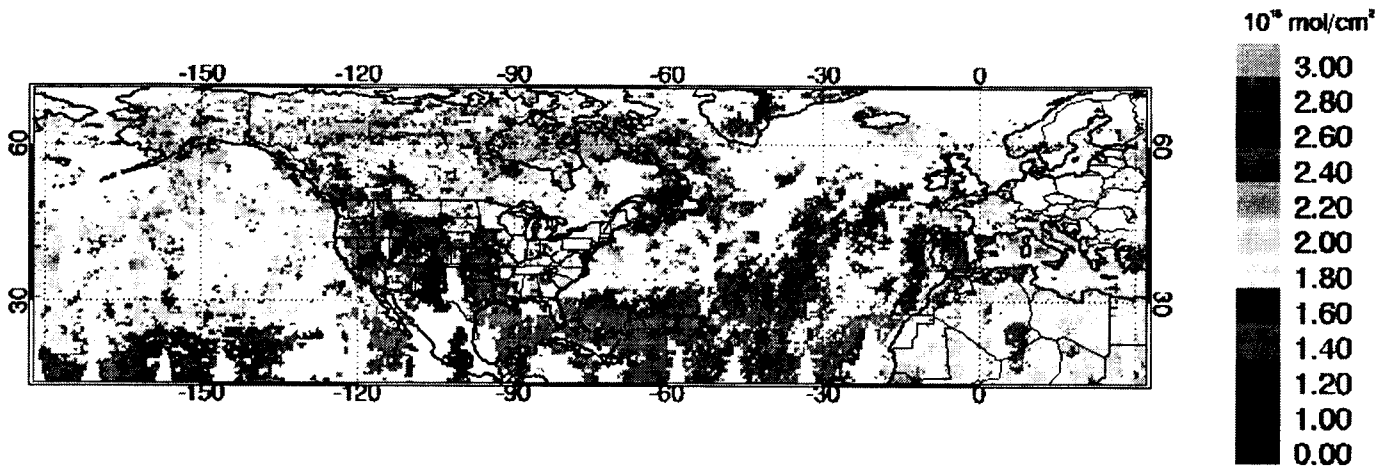


[Send comments to Web Learner](#)



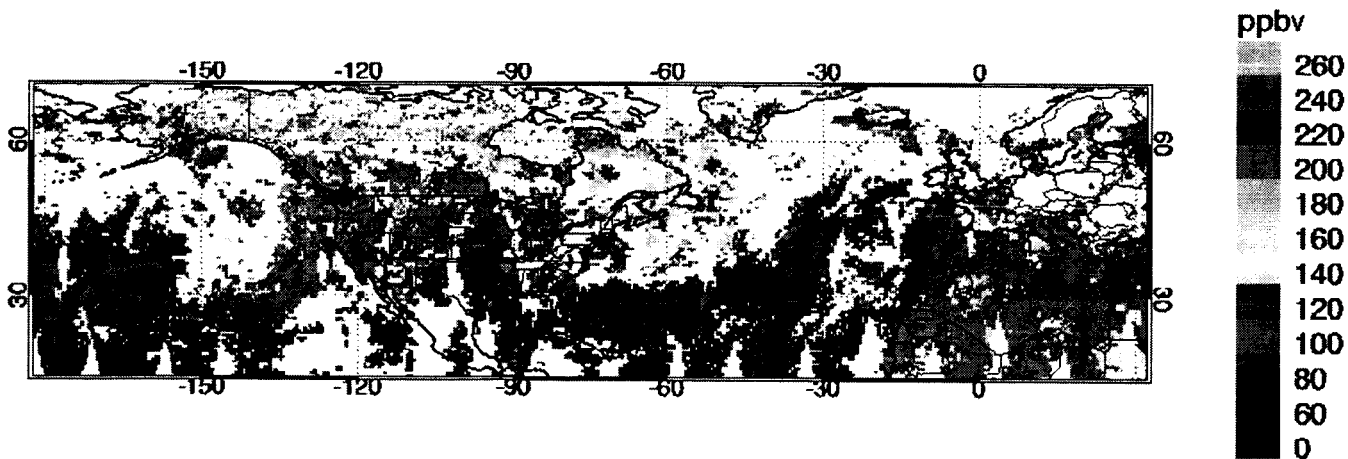
3-Day Field Project Region Plots for 2004-07-12 through 2004-07-14

MOPITT CO (V3) Column Jul 12, 2004-Jul 14, 2004



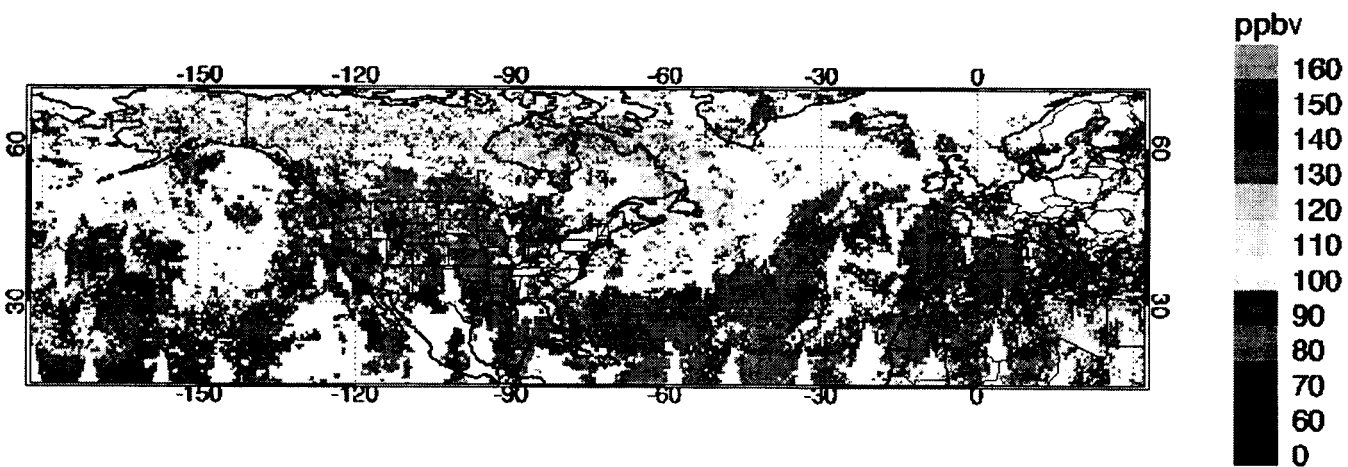
Gridded at 0.5x0.5deg from MOP02-20040714-L2V5.9.4.prov.hdf (apriori fraction < 50%)

MOPITT CO (V3) 700hPa Jul 12, 2004-Jul 14, 2004

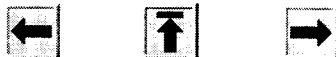


Gridded at 0.5x0.5deg from MOP02-20040714-L2V5.9.4.prov.hdf (apriori fraction < 50%)

MOPITT CO (V3) 350hPa Jul 12, 2004-Jul 14, 2004



Gridded at 0.5x0.5deg from MOP02-20040714-L2V5.9.4.prov.hdf (apriori fraction < 50%)



[Send comments to Web Learner](#)

Quantifying CO emissions from the 2004 Alaskan wildfires using MOPITT CO data

G. Pfister,^{1,2} P. G. Hess,¹ L. K. Emmons,¹ J.-F. Lamarque,¹ C. Wiedinmyer,¹
D. P. Edwards,¹ G. Pétron,^{1,2} J. C. Gille,¹ and G. W. Sachse³

Received 15 March 2005; revised 22 April 2005; accepted 18 May 2005; published 14 June 2005.

[1] We present an inverse model analysis to quantify the emissions of wildfires in Alaska and Canada in the summer of 2004 using carbon monoxide (CO) data from the Measurements of Pollution in the Troposphere (MOPITT) remote sensing instrument together with the chemistry transport model MOZART (Model for Ozone and Related Chemical Tracers). We use data assimilation outside the region of the fires to optimally constrain the CO background level and the transport into that region. Inverse modeling is applied locally to quantify the fire emissions. Our a posteriori estimate of the wildfire emissions gives a total of 30 ± 5 Tg CO emitted during June–August 2004 which is of comparable order to the anthropogenic emissions for the continental US. The simulated CO fields have been evaluated by comparison with MOPITT and independent aircraft data. **Citation:** Pfister, G., P. G. Hess, L. K. Emmons, J.-F. Lamarque, C. Wiedinmyer, D. P. Edwards, G. Pétron, J. C. Gille, and G. W. Sachse (2005), Quantifying CO emissions from the 2004 Alaskan wildfires using MOPITT CO data, *Geophys. Res. Lett.*, 32, L11809, doi:10.1029/2005GL022995.

1. Introduction

[2] CO plays a central role in atmospheric chemistry by acting as a major sink for hydroxyl radicals and through its role in the production of ozone. Significant uncertainties still persist in regional estimates of CO emissions, leading to key uncertainties in the impact of human and natural activities on the atmospheric distribution of CO. Two different approaches are widely used to estimate the emissions of atmospheric trace gases: bottom-up estimates (i.e. techniques applying emission factors to socioeconomic, energy, land use, and environmental data) and top-down estimates using observational data (i.e. inverse modeling approaches). Bayesian synthesis inversion techniques have been applied in various studies of the CO budget [e.g., Bergamaschi *et al.*, 2000; Arellano *et al.*, 2004; Pétron *et al.*, 2004; Heald *et al.*, 2004]. All of these studies identify significant differences between top-down and bottom-up emission estimates.

[3] We present a top-down constraint on CO emissions from the wildfires in Alaska and Canada in summer 2004.

¹Atmospheric Chemistry Division, National Center for Atmospheric Research, Boulder, Colorado, USA.

²Also at Advanced Study Program, National Center for Atmospheric Research, Boulder, Colorado, USA.

³NASA Langley Research Center, Hampton, Virginia, USA.

The fires that burned from mid-June until September were the largest on record for Alaska. We apply a Bayesian inverse technique using MOPITT observations of CO, daily a priori bottom-up emission estimates based on MODIS (Moderate Resolution Imaging Spectroradiometer) fire counts, and the chemical transport model MOZART. In the evaluation of the a posteriori emissions we use MOPITT CO data and aircraft observations from the INTEX-NA (Intercontinental Chemical Transport Experiment – North America) campaign.

2. Methodology

[4] We apply an inverse technique to seek an optimal solution for trace gas emissions consistent with both the observed atmospheric constraints and the a priori emissions estimate. When solving for emissions within a selected region the emitted contribution to the CO budget within the region needs to be differentiated from the contribution from outside the region. In this study, we account for CO that is transported into the region of the fires by assimilating MOPITT CO data into MOZART outside the impacted region. This methodology provides constraints on the CO transported into the domain with high spatial and temporal resolution and compared to optimizing emissions on a global basis it is less affected by model transport errors. We assume that within the region of interest the differences between MOPITT and modeled CO are predominantly due to local fire emissions. It is these differences we use to optimally infer the fire emissions.

[5] The methodology requires the following components: an a priori estimate of the fire emissions, a forward model to relate the estimated CO emissions to the measurements, CO measurements, an assimilation scheme, and an inverse modeling approach. Each component is discussed below.

2.1. Model A Priori Emissions

[6] The a priori fire emissions for Alaska and Canada as well as fire emissions for the rest of North America are derived from MODIS fire counts (as by Giglio *et al.* [2003]). The land cover burned is based on the Global Land Cover 2000 data set (<http://www.gvm.jrc.it/glc2000>) and the MODIS Vegetation Continuous Fields product [DeFries *et al.*, 2000]. Emission factors from literature have been assigned to the land cover biomass [e.g., Battye and Battye, 2002; Andreae and Merlet, 2001], and assumptions of fuel consumption are based on Ito and Penner [2004]. The fire emissions for North America are provided as daily means.

[7] The a priori biomass burning emissions over the Alaskan-Canadian region total 13 Tg CO for June through

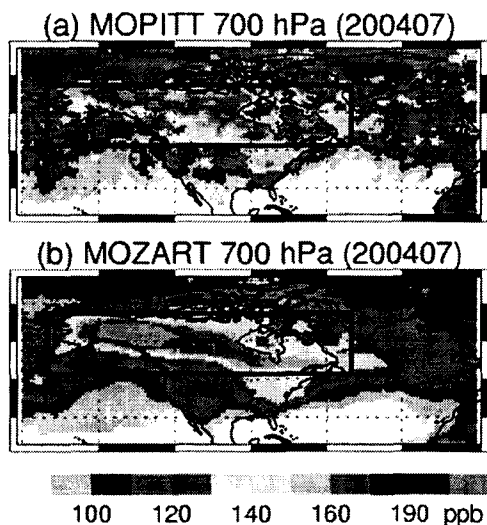


Figure 1. (a) MOPITT and (b) MOZART CO mixing ratio at 700 hPa averaged for July 2004. The box defines the region used in the optimization. Outside the box the modeled CO fields are constrained by data assimilation, inside the box the CO fields are optimized by inverse modeling. The MOPITT data have been averaged over a 1° by 1° grid and the monthly mean averaging kernels have then been applied to the nearest model profile.

August. As defined by the variation in the fire counts, the fire emissions have a strong temporal and spatial variability compared to other sources. Anthropogenic CO emissions [Olivier *et al.*, 2003] in the selected region are 1.5 Tg for June through August, and CO from biogenic sources [Müller, 1992] is 5 Tg.

2.2. The Forward Model

[8] The global chemistry transport model MOZART [Horowitz *et al.*, 2003] is used as the forward model. The simulation is driven by meteorological fields from the National Centers for Environmental Prediction (NCEP) re-analysis with 6 hours resolution. The spatial resolution of the model is $\sim 2.8^\circ \times 2.8^\circ$ with 28 levels in the vertical (17 levels between the surface and 200 hPa). The chemical time step of the model is 20 minutes.

[9] Modifications in the model from the version published by Horowitz *et al.* [2003] include an online dry deposition scheme based on Wesley [1989], the interactive calculation of isoprene and soil NO_x emissions, updates in the chemical scheme, and fixed surface concentrations of methane constrained by CMDL observations. Further information can be found on the MOZART webpage (www.acd.ucar.edu/science/gctm/mozart).

2.3. MOPITT CO Data

[10] MOPITT is a nadir IR correlation radiometer aboard the NASA Terra satellite. The Level 2 V3 MOPITT dataset consists of retrieved CO mixing ratios for 7 vertical levels in the atmosphere (surface to 150 hPa). However, the number of independent pieces of information in one profile is typically less than 2 [Deeter *et al.*, 2004]. The MOPITT retrievals show

strongest sensitivity in the middle troposphere [Deeter *et al.*, 2003], where the main transport of CO from the fires takes place, but they have low sensitivity to the boundary layer. The latter implies that the MOPITT observations could underestimate emissions by only accounting for emissions that reach the free troposphere.

[11] We restrict our analysis to MOPITT retrievals with an a priori contribution of less than 50% to ensure that the measurements used are representative of observed CO rather than MOPITT a priori information [Deeter *et al.*, 2004]. MOPITT validation for data after August 2001 shows a small bias (≤ 1 ppb) at all altitudes with a standard deviation of ~ 20 ppb [Emmons *et al.*, 2004]. For information about the MOPITT measurement and validation we refer to Deeter *et al.* [2003] and Emmons *et al.* [2004].

2.4. Data Assimilation

[12] The data assimilation scheme for MOPITT CO is based on the 3D suboptimal Kalman filter scheme described by Lamarque *et al.* [1999] and Khattatov *et al.* [2000]. Only MOPITT data south of 70N are used to ensure sufficient sensitivity of the MOPITT retrieval to the atmospheric CO profile. We apply data assimilation outside the region largely impacted by the wildfires. Within the region we calculate the observed *minus* forecast (OMF) CO using data assimilation, but do not update the CO fields. The impacted region is defined from 47N to 71N and 170W to 50W and covers the location of the fires as well as the main outflow. Figure 1a shows the selected region overlaid on a MOPITT composite. The composite illustrates the large amounts of CO released by the wildfires and the widespread transport of pollution associated with them. We begin the simulations in April 2004 to allow sufficient time for the assimilation procedure to reduce the model-measurement bias.

2.5. Inverse Modeling

[13] The inverse technique relates a measurement vector \mathbf{y} to individual CO sources (assembled in a state vector \mathbf{x}) via the Jacobian matrix \mathbf{K} and an error vector $\boldsymbol{\epsilon}$: $\mathbf{y} = \mathbf{K}\mathbf{x} + \boldsymbol{\epsilon}$ [Rodgers, 2000]. \mathbf{K} describes the sensitivity of \mathbf{y} to finite changes in \mathbf{x} and $\boldsymbol{\epsilon}$ represents the total observational error. We do not invert for the spatial distribution of the emissions, but invert for their strength on a weekly timescale from June until the first week in September 2004. The resulting 14 source categories (one for each week) are included as additional species ("tagged CO") in the full chemistry version of the model. The inversion is iterated three times and the OH fields adjusted for the updated fire emissions. The errors in the a priori emissions are assumed to be uncorrelated and are set to 100% based on comparisons of emission estimates for other fires. The observational error is assumed equal to the variance in the data assimilation (50%).

[14] In this methodology we assume that the OMF is a representative estimate of the adjustment that has to be applied to the a priori emissions to match the modeled with the observed CO. That is, we assume that contributions to CO from other sources within the selected region are small compared to the fires (e.g. anthropogenic emissions) and/or reasonably well known (e.g. CO produced from methane oxidation). The OMF prior to the start of the wildfires supports this assumption. The mean OMF for May 2004

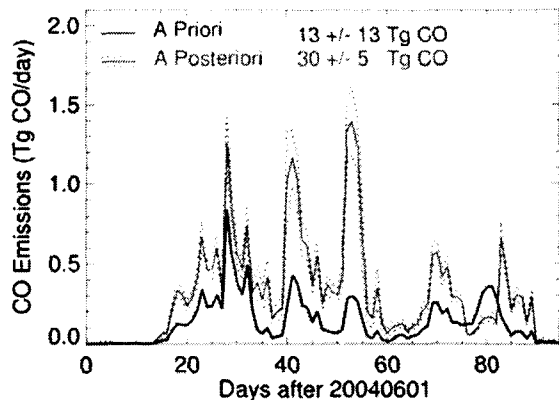


Figure 2. A priori and a posteriori emission estimates for June–August 2004 from the wildfires. Solid lines indicate the mean value, dotted lines the $1\text{-}\sigma$ uncertainty.

averaged over Alaska/Canada is 4 ± 2 ppb CO at 850 hPa, 1 ± 1 ppb at 500 hPa, 0 ± 1 ppb at 250 hPa.

[15] The MOPITT levels at 850 hPa and 700 hPa are used in independent inversions because they are most sensitive to the lowermost atmospheric CO concentrations. The MOPITT surface retrieval level has not been used because of its large a priori contribution at high latitudes. The averaging kernels of the inversion [Rodgers, 2000] indicate 11 independent pieces of information were used in the inversion of the weekly fire emissions. The chi-square of the inversion is 0.96.

3. Results

[16] We only invert for the near-field response to the fires because the CO outside the domain is constrained by the assimilation. To ensure this, we set the concentrations of the fire tracers to zero outside the region of interest so that they are not transported back into the domain. The CO fire emissions are distributed homogeneously with regard to number density between the surface and 400 hPa to account for fire-related convection. The modeled CO fields for July 2004 after the third iteration show good agreement with the MOPITT CO (Figure 1b). MOPITT shows a more pronounced spatial structure compared to the model which is due to the coarser model resolution (see figure caption) and presumably also due to varying emission injection heights that are not reproduced in the model. Discrepancies are further explained by uncertainties in the spatial distribution of the fire location, uncertainties in local emissions other than fires, and model transport errors.

[17] Figure 2 shows the time series for the a priori and a posteriori fire emissions. The a posteriori estimate for the CO emitted by the fires for June–August 2004 is 30 ± 5 Tg CO, over twice the a priori estimate. The average a posteriori error calculated from the inversion [Rodgers, 2000] is 18%, however for individual weekly sources the error varies between 13% and 100% (the latter for the first two weeks in June and the first week in September). Due to the uncertainty in injection height, another inversion was performed for comparison in which the fire emissions were emitted at the lowermost model layer, and distributed

in the boundary layer by the model boundary layer scheme. This showed no strong impact on the derived emissions strength.

[18] A priori and a posteriori emissions show a remarkable correlation in time except at the end of August where the a posteriori emissions peak a few days after the a priori emissions. It is interesting to see that as summertime advances the adjustment to the a priori emissions increases. This might be due to peat fires which are known for releasing large amounts of CO into the atmosphere [Christian *et al.*, 2003]. Peat fires could be gaining in intensity and frequency when frozen surface layers are warming up, however, further investigations are needed to support this hypothesis.

[19] The OMF for June to August remaining after the third iteration is about 2 ± 3 ppb CO at 850 hPa, -1 ± 3 ppb at 500 hPa, and -1 ± 2 ppb at 250 hPa. This is similar to the range of the OMF for May 2004 (Section 2.5).

4. Evaluation

[20] To evaluate the fire emissions, we performed reference runs with a priori and a posteriori fire emissions, respectively, and without data assimilation, and compared these simulations with observed CO fields. The fire emissions for NO_x and hydrocarbons were increased by the same factor as the CO emissions. A comparison of the reference runs shows that the increase in the tropospheric column of ozone due to the increase in the fire emissions can be as high as 25% in the vicinity of the fires and as high as 10% over Europe.

[21] Table 1 shows the mean bias and standard deviation of MOPITT CO minus modeled CO for the reference runs. The bias is clearly reduced when using the a posteriori emissions, not only over the region of the wildfires but also outside the domain. The rather high bias that remains in the case of the a posteriori emissions is due to the fact that the background CO levels in the reference runs are too low as these runs do not use data assimilation to adjust the transport into the impacted region. The burden of CO in the reference runs over Canada/Alaska is 7 Tg in May 2004 and increases to 10 Tg CO when data assimilation is applied outside the domain.

[22] We further evaluated the model results by comparison with aircraft observations of CO [Sachse *et al.*, 1987] from INTEX-NA. INTEX-NA took place from end of June until middle of August with flights over the US-West Coast, Mid-America, and New England. Here we examine flights in the vicinity of the New England area as this is the sampled region most affected by the fires. Each of the

Table 1. Mean Bias and Standard Deviation (ppb) of MOPITT Minus Model CO for the Region of the Source Optimization and a Region Downwind ($50\text{--}70\text{N}$, $50\text{--}20\text{W}$)^a

	Alaska/Canada		Atlantic	
	A Priori	A Posteriori	A Priori	A Posteriori
850 hPa	29 ± 22	18 ± 23	25 ± 13	14 ± 13
500 hPa	12 ± 9	7 ± 9	8 ± 5	4 ± 5
250 hPa	6 ± 6	3 ± 7	4 ± 5	1 ± 5

^aResults for three retrieval levels are shown.

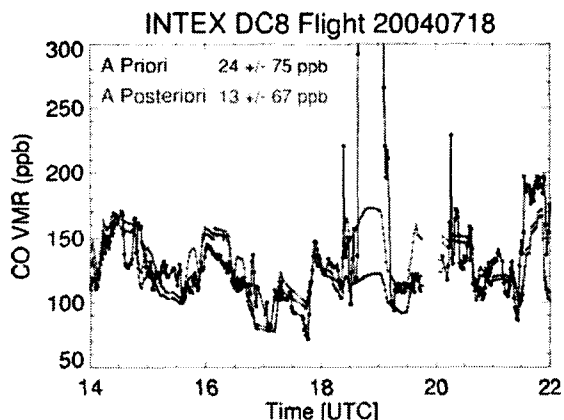


Figure 3. Observed and modeled (a priori and a posteriori) CO time series for the flight on July 18, 2004. The plume observed at 18–19 UTC has values up to 600 ppb (for clarity scale has been reduced).

8 flights examined lasted about 8 hours and covered an altitude range from the surface up to 10 km above ground level.

[23] We use 1-minute averages of the observations and compare them to the corresponding 3-hour average CO concentrations from the model. The uncertainty for the aircraft data is given as 2% or 2 ppb. The model data have been spatially interpolated to the location of the observations. For all flights the mean bias is 8 ± 42 ppb with the a priori emissions and 1 ± 40 ppb with the a posteriori emissions. The correlation coefficients are 0.44 and 0.53, respectively.

[24] Figure 3 shows the modeled and measured CO time series for the flight on 18 July 2004 which was flown out of Pease to the northeast over the Island of Newfoundland. This was the flight most impacted by the wildfires with measured CO mixing ratios as high as 600 ppb at 400 hPa. Although the model cannot replicate the measured magnitude of this intense plume because of its coarser resolution, the timing and location of the plume are well reproduced, and the model-measurement agreement is clearly improved using the a posteriori emissions. Without this intense plume event the comparison for the remaining flights is 5 ± 33 ppb for the a priori, and 0 ± 33 ppb for the a posteriori emissions.

5. Summary

[25] We present an inverse modeling study to constrain the emissions of the wildfires in Alaska and Canada in summer 2004. Our best guess of the fire emissions is 30 ± 5 Tg CO for June–August 2004, which is on the order of the anthropogenic CO emissions for the entire continental US for the same time period (~ 25 Tg CO).

[26] In contrast to other top-down inverse modeling studies, we apply data assimilation outside the region of interest to minimize uncertainties in the background CO. This represents an advantage over other approaches when considering isolated emission sources because of minimizing the model transport error and because of constraining

the contribution of CO transported into the region of interest with high temporal and spatial resolution.

[27] The vertical distribution of the fire emissions of CO had no significant impact on the derived source strength in our study, but a more comprehensive analysis will be needed in order to understand the impact of fire-related convection.

[28] **Acknowledgments.** The authors thank the MOPITT and INTEX-NA Teams for support with CO data and Greg Frost and Stu McKeen for providing access to the EPA emission database. We acknowledge Valery Yudin, Frank Flocke, William Randel, Paul Palmer and an anonymous reviewer for valuable input to this manuscript. This work was supported by NASA grants EOS/03-0601-0145 and NNG04GA459. NCAR is operated by the University Corporation of Atmospheric Research under sponsorship of the National Science Foundation.

References

- Andreae, M. O., and P. Merlet (2001), Emission of trace gases and aerosols from biomass burning, *Global Biogeochem. Cycles*, *15*, 955–966.
- Arellano, A. F., Jr., P. S. Kasibhatla, L. Giglio, G. R. van der Werf, and J. T. Randerson (2004), Top-down estimates of global CO sources using MOPITT measurements, *Geophys. Res. Lett.*, *31*, L01104, doi:10.1029/2003GL018609.
- Battye, W., and R. Battye (2002), Development of emissions inventory methods for wildland fire, final report, EPA contract 68-D-98-046, U.S. Environ. Prot. Agency, Rectangle Park, N. C. (<http://www.epa.gov/ttn/chief/ap42/ch13/related/firerept.pdf>)
- Bergamaschi, P., R. Hein, M. Heimann, and P. J. Crutzen (2000), Inverse modeling of the global CO cycle: 1. Inversion of CO mixing ratios, *J. Geophys. Res.*, *105*, 1909–1928.
- Christian, T. J., B. Kleiss, R. J. Yokelson, R. Holzinger, P. J. Crutzen, W. M. Hao, B. H. Saharjo, and D. E. Ward (2003), Comprehensive laboratory measurements of biomass burning emissions: Emissions from Indonesian, African, and other fuels, *J. Geophys. Res.*, *108*(D23), 4719, doi:10.1029/2003JD003704.
- Deeter, M. N., et al. (2003), Operational carbon monoxide retrieval algorithm and selected results for the MOPITT instrument, *J. Geophys. Res.*, *108*(D14), 4399, doi:10.1029/2002JD003186.
- Deeter, M. N., L. K. Emmons, D. P. Edwards, J. C. Gille, and J. R. Drummond (2004), Vertical resolution and information content of CO profiles retrieved by MOPITT, *Geophys. Res. Lett.*, *31*, L15112, doi:10.1029/2004GL020235.
- DeFries, R., M. Hansen, J. R. G. Townshend, A. C. Janetos, and T. R. Loveland (2000), *Continuous Fields 1 Km Tree Cover*, Global Land Cover Facil., College Park, Md.
- Emmons, L. K., et al. (2004), Validation of Measurements of Pollution in the Troposphere (MOPITT) CO retrievals with aircraft in situ profiles, *J. Geophys. Res.*, *109*, D03309, doi:10.1029/2003JD004101.
- Giglio, L., J. Descloitres, C. O. Justice, and Y. J. Kaufman (2003), An enhanced contextual fire detection algorithm for MODIS, *Remote Sens. Environ.*, *87*, 273–282.
- Heald, C. L., D. J. Jacob, D. B. A. Jones, P. I. Palmer, J. A. Logan, D. G. Streets, G. W. Sachse, J. C. Gille, R. N. Hoffman, and T. Nehrkorn (2004), Comparative inverse analysis of satellite (MOPITT) and aircraft (TRACE-P) observations to estimate Asian sources of carbon monoxide, *J. Geophys. Res.*, *109*, D23306, doi:10.1029/2004JD005185.
- Horowitz, L. W., et al. (2003), A global simulation of tropospheric ozone and related tracers: Description and evaluation of MOZART, version 2, *J. Geophys. Res.*, *108*(D24), 4784, doi:10.1029/2002JD002853.
- Ito, A., and J. E. Penner (2004), Global estimates of biomass burning emissions based on satellite imagery for the year 2000, *J. Geophys. Res.*, *109*, D14S05, doi:10.1029/2003JD004423.
- Khattatov, B. V., J.-F. Lamarque, L. V. Lyjak, R. Menard, P. Levelt, X. Tie, G. P. Brasseur, and J. C. Gille (2000), Assimilation of satellite observations of long-lived chemical species in global chemistry transport models, *J. Geophys. Res.*, *105*, 29,135–29,144.
- Lamarque, J.-F., B. V. Khattatov, J. C. Gille, and G. P. Brasseur (1999), Assimilation of Measurement of Air Pollution from Space (MAPS) CO in a global three-dimensional model, *J. Geophys. Res.*, *104*, 26,209–26,218.
- Müller, J.-F. (1992), Geographical distribution and seasonal variation of surface emissions and deposition velocities of atmospheric trace gases, *J. Geophys. Res.*, *97*, 3787–3804.

- Olivier, J., J. Peters, C. Granier, G. Petron, J. F. Müller, and S. Wallens (2003), Present and future surface emissions of atmospheric compounds, POET Rep. 2, Eur. Union, Brussels.
- Pétron, G., C. Granier, B. Khattatov, V. Yudin, J.-F. Lamarque, L. Emmons, J. Gille, and D. P. Edwards (2004), Monthly CO surface sources inventory based on the 2000–2001 MOPITT satellite data, *Geophys. Res. Lett.*, *31*, L21107, doi:10.1029/2004GL020560.
- Rodgers, C. (2000), *Inverse Methods for Atmospheric Sounding: Theory and Practice*, World Sci., Hackensack, N. J.
- Sachse, G. W., G. F. Hill, L. O. Wade, and M. G. Perry (1987), Fast-response, high precision carbon monoxide sensor using a tunable diode laser absorption technique, *J. Geophys. Res.*, *92*, 2071–2081.
- Wesley, M. L. (1989), Parameterization of surface resistance to gaseous dry deposition in regional-scale numerical models, *Atmos. Environ.*, *23*, 1293–1304.
-
- D. P. Edwards, L. K. Emmons, J. C. Gille, P. G. Hess, J.-F. Lamarque, G. Pétron, G. Pfister, and C. Wiedinmyer, Atmospheric Chemistry Division, National Center for Atmospheric Research, P.O. Box 3000, Boulder, CO 80307–3000, USA. (pfister@ucar.edu)
- G. W. Sachse, NASA Langley Research Center, Mail Stop 472, Hampton, VA 23681–2199, USA.